Journal of Applied Physics

Composition and lattice-mismatch measurement of thin semiconductor layers by x-ray diffraction

Cite as: Journal of Applied Physics **62**, 4154 (1987); https://doi.org/10.1063/1.339133
Submitted: 13 April 1987 . Accepted: 05 August 1987 . Published Online: 04 June 1998

P. F. Fewster, and C. J. Curling

Composition and lattice-mismatch measurement of thin semiconductor layers by x-ray diffraction

P. F. Fewster and C. J. Curling
Philips Research Laboratories, Redhill, Surrey, England

(Received 13 April 1987; accepted for publication 5 August 1987)

X-ray diffraction methods for determining alloy composition and mismatch have been used for many years by measuring the separation of peaks in a high-resolution diffractogram. This method can still be used, but not for layer thicknesses below 1–2 μm. The diffractogram may appear simple to interpret, for example, two diffraction peaks from a single layer on a substrate, but simple measurement of peak separation can lead to significant errors in determining the mismatch and hence alloy composition. This paper gives examples of peak shifting with thin layers and shows how, by simulating the diffraction profiles, a reliable determination of mismatch, and hence alloy composition can be made.

I. INTRODUCTION

X-ray diffraction is commonly used for the composition measurement of closely lattice-matched thin epitaxially grown semiconductor layers on thick substrates.[1–3] The method is relatively simple in that it involves the measurement of the peak separation in a high-resolution diffractogram and calculation, taking into account layer distortion effects. This method will be briefly reviewed, as well as the conditions when this approach is no longer valid.

Many structures of interest today involve thin layers, and if many thin layers are involved, the diffraction profiles become complex and simple analysis is no longer applicable.[3,4] The only way to interpret such profiles is by simulation.[5,6]

For simple structures it is still tempting to use the simple approach, if the peaks are well defined. This paper will indicate the limitations and problems encountered with this method for the $Al_xGa_{1-x}As/GaAs$ system, although the conclusions are general. An example of peak shifting for an $In_xGa_{1-x}As$ layer on an InP substrate is also given.

II. METHOD

The diffraction profiles for the accurate determination of alloy composition or mismatch are usually obtained on a double-crystal diffractometer. Generally, the substrate and layer peaks in the diffraction profile can be labeled and their separation determined.[2,3,7,8] The angular separation of the peaks, $\Delta\omega$, can be related to the lattice mismatch through the differential form of Bragg's Law

$$(\Delta a/a)_\perp = -\cot\theta\Delta\omega/\cos^2\phi, \tag{1}$$

where θ is the Bragg angle and $\cos^2\phi$ accounts for diffraction from planes inclined at ϕ from the crystal surface. $(\Delta a/a)_\perp$ represents the mismatch perpendicular to the crystal surface, which relates to the "relaxed" lattice mismatch $(\Delta a/a)_R$, provided the interfacial misfit dislocation density is low ($< 10^3\ \mathrm{cm}^{-2}$), by

$$\left(\frac{\Delta a}{a}\right)_r = \left(\frac{\Delta a}{a}\right)_\perp \left(\frac{1-\nu}{1+\nu}\right), \tag{2}$$

where ν is Poisson's ratio for the layer material. This "relaxed" mismatch can then be related to the alloy composition by Vegard's Law.

Clearly, in deriving Eq. (1) we have assumed that the layer and substrate diffract x rays independently. We have assumed that the same peak position (ignoring effects due to elastic deformation) would be obtained for a thin crystal compared with a thin crystal layer on a closely matched substrate. This does not account for the different boundary conditions at the undersurface of the thin crystal compared with that for a layer on a substrate. Because we have ignored the influence of the beam entering the substrate we cannot be sure that the angular separation will give a true value for the mismatch. To ensure that the influence of this boundary condition is included, we can simulate the profile and compare the peak separation of the layer and substrate with respect to the separation obtained when both layer and substrate diffract x rays independently. The solution of the Takagi–Taupin equations,[5,6] which represent a two-beam dynamical scattering approach with the introduction of a deviation parameter

$$\alpha_h(\omega) = -2\lambda(\theta-\theta_0)\cos\theta_0/d,$$

where d is the interplane spacing and θ_0 is the Bragg angle for the substrate or layer, will allow modeling of such structures. $\alpha_H(\omega)$ purely represents the angular deviation from the Bragg angle for which the calculated amplitude ratio is required, where the Bragg angle and d are the values for the region in the crystal at which this ratio is calculated. This deviation parameter is valid for angular ranges of a few degrees either side of the Bragg angle. The basic equations are:

$$\frac{i\lambda\gamma_H}{\pi}\frac{dD_H}{dz} = \Psi_0 D_H + C\Psi_H D_0 - \alpha_H(\omega)D_H,$$
$$\frac{i\lambda\gamma_0}{\pi}\frac{dD_0}{dz} = \Psi_0 D_0 + C\Psi_{\bar{H}} D_H, \tag{3}$$

where D_0 and D_H are the incident and diffracted amplitudes, and z is the depth into the crystal. $\gamma_H = \mathbf{n}\cdot\mathbf{k}_H$, where $\mathbf{n}$ is the surface normal and $\mathbf{k}$ is the diffracted beam vector, λ is the wavelength, C is the polarization factor ($= 1$ or $|\cos 2\theta|$), and Ψ_H is related to the structure factor F_H by

$$\Psi_H = (\lambda^2 r_e/\pi V)F_H,$$

 0021-8979/87/224154-05$02.40

where V is the unit cell volume and r_e is the electron radius. If we define an amplitude ratio $X = D_H/D_0$ then these combine to give

$$\frac{dX}{dz} = -\frac{i\Pi}{\lambda\gamma_H}\left\{\Psi_H - \Psi_{\bar{H}}\left(\frac{|\gamma_H|}{\gamma_0}\right)X^2 + \left[\Psi_0\left(1 - \frac{|\gamma_H|}{\gamma_0}\right) - \alpha_H(\omega)\right]X\right\} \quad (4)$$

which can be integrated after separation into partial fractions. This is a standard integral and its solution is given by

$$X(Z,\omega) = \frac{SX(z,\omega) + i[E + BX(z,\omega)]\tan GS(z-Z)}{S - i[AX(z,\omega) + B]\tan GS(z-Z)}, \quad (5)$$

where

$$A = \Psi_{\bar{H}}|\gamma_H|/\gamma_0,$$
$$B = 0.5[\Psi_0(1 - |\gamma_H|/\gamma_0) - \alpha_H(\omega)],$$
$$S = (B^2 - AE)^{1/2},$$
$$G = -\pi/(\lambda|\gamma_H|),$$
$$E = \Psi_H.$$

The boundary condition can then be that the substrate is thick enough such that the reflectivity deep inside the crystal $X(\infty,\omega) = 0$. Hence, we determine the reflectivity at the surface of the substrate.[9] This amplitude ratio is then the boundary condition for the undersurface of the first layer of depth z and the thickness t to obtain $X(z-t,\omega)$ at the top of the first layer. The procedure is repeated until $X(0,\omega)$ at the surface of the structure is obtained. The reflectivity is therefore given by

$$R(\omega) = X(0,\omega)X^*(0,\omega)(|\gamma_H|/|\gamma_0|). \quad (6)$$

This is calculated for the angular range $(\omega_1 - \omega_2)$ of the experiment.

III. DISCUSSION

Two types of structures are considered to illustrate the importance of modeling profiles for obtaining accurate values of mismatch and hence composition.[10]

A. Structure type I

This is simply a single $Al_{0.5}Ga_{0.5}As$ layer on a GaAs substrate. The diffraction profiles are calculated for various layer thicknesses and the peak separation determined for the 004 reflection with Cu$K\alpha$ radiation. The calculated diffraction profiles are given in Fig. 1. The peak separations, assuming the main feature (apart from the substrate) is that from the layer, are plotted in Fig. 2 as a function of layer thickness.

The layer peak clearly is drawn towards the substrate as the thickness is reduced below $\sim 0.5\ \mu$m until eventually it appears as an asymmetric broadening of the substrate peak. Before this stage we could go for an asymmetric reflection, e.g., 115 (whose profiles are not illustrated) or 224 to geometrically enhance the scattering from the layer (Fig. 3). Again we observe a similar effect occurring for thicknesses below $\sim 0.5\ \mu$m for the 224 reflection (Fig. 2), therefore, although the reflectivity is enhanced in using asymmetric diffracting planes, the peak shifting is still present. The mismatch derived, and hence the alloy composition, from such a profile is clearly underestimated if it is derived from Eq. (1) and the separation of peaks, although the diffraction profiles appear to be easily interpretable by standard means.

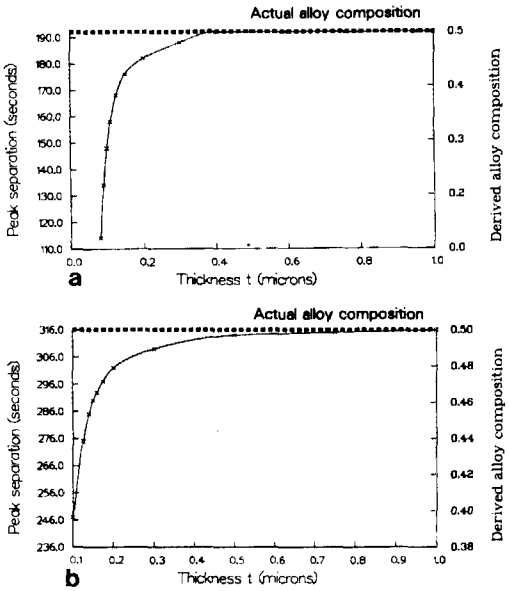

FIG. 2. The variation in peak separation (and its derived alloy composition) for various thicknesses of a single $Al_{0.5}Ga_{0.5}As$ layer compared with the actual alloy composition for the (a) 004 and (b) 224 reflections.

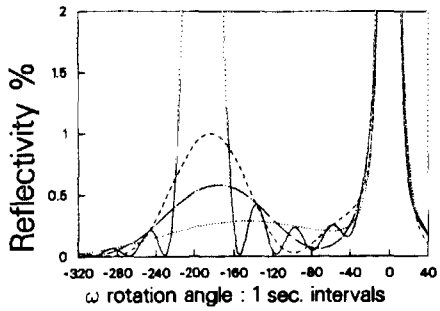

FIG. 1. Simulated diffraction profiles of the 004 reflection (Cu$K\alpha$) for a single $Al_{0.5}Ga_{0.5}As$ layer of thickness t on a GaAs substrate. $t = 0.5$ (solid), 0.2 (dash), 0.15 (dot-dash), and 0.1 (dot) μm.

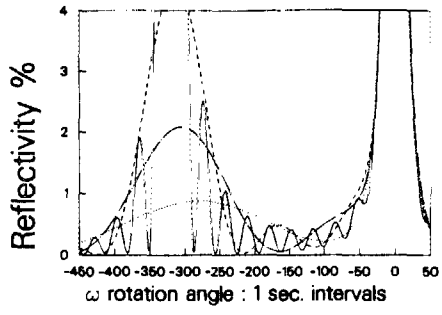

FIG. 3. Simulated diffraction profiles of the 224 reflection (Cu$K\alpha$) for a single $Al_{0.5}Ga_{0.5}As$ layer of thickness t on a GaAs substrate. $t = 1$ (solid), 0.3 (dash), 0.2 (dot-dash), and 0.125 (dot) μm.

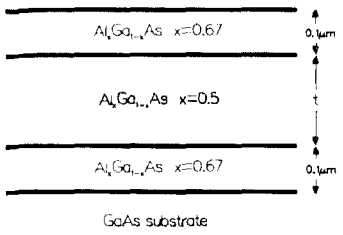

FIG. 4. The dimensions of the structural type II, which has been simulated for different "sandwich" layer thicknesses, t.

B. Structure type II

This is a "sandwich" structure given in Fig. 4, which clearly brings in more variables to influence the profile. Computer simulated profiles for the two reflections, 004 and 224, have been calculated for a range of thicknesses (Figs. 5 and 6). Clearly in this case where we have thin cladding regions, 0.1 μm, we might expect the main peak, apart from that from the substrate, to give a good value for the mismatch of the "sandwich" layer. The plots of peak shift versus layer thickness do, though, indicate that if the layer is less than $\sim 2\,\mu$m thick for any of these reflections, then this principal peak shifts away from the expected position and will give an overestimate for the mismatch (Fig. 7). Of course, this is not too surprising for cladding layers which are a significant proportion of the total thickness, but in Fig. 7 we can see that there is a monotonic increase in the peak separation with decreasing layer thickness below $\sim 2\,\mu$m for 0.1-μm claddings, until eventually a peak corresponding to 0.2 μm (the sum of the two cladding thicknesses) emerges.

Suppose now we have a different situation where the cladding layers are thicker (1 μm); then we see that the major peaks apart from that of the substrate are split and the peak between arises from the "sandwiched" layer (Fig. 8). On decreasing the layer thickness from 2 to 0.4 μm, we observe a shift in this peak to give an overestimate of the mismatch and hence alloy composition. At 0.4 μm the peak shape is complex, but when convoluted with the instrument function if the resolution is not too high, then this can appear as a broad single peak. Above 2 μm the peak does not shift and below 0.4 it no longer becomes resolved. The peaks associated with the cladding layers are very complex, making measurement of that composition very indeterminant from inspection, but this interference effect clearly gives a sensitive measure of the cladding layer separation.

At this point we can clearly see that for thin single layers

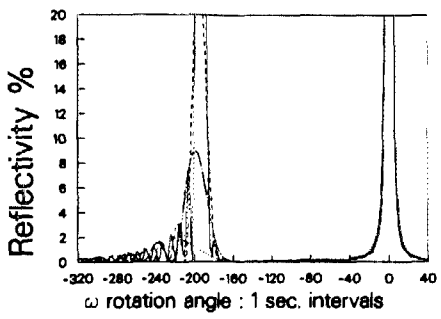

FIG. 5. Simulated profiles of the type II structure (Fig. 4), 004 reflection (Cu$K\alpha$) for $t = 2$ (solid), 1 (dash), 0.5 (dot-dash), and 0.1 (dot) μm.

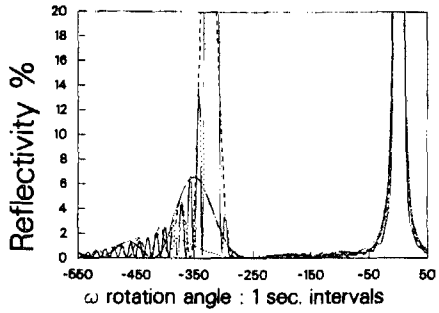

FIG. 6. Simulated profiles of the type II structure (Fig. 4), 224 reflection (Cu$K\alpha$) for $t = 2$ (solid), 0.75 (dash), 0.2 (dot-dash), and 0.001 (dot) μm.

the peak separation decreases as its thickness is reduced, and for a "sandwiched" layer the peak separation increases with decreasing thickness. However, if we follow the peak separation as the cladding layers are increased in thickness, then the peak separation from the "sandwiched" layer to the substrate should increase from a value below that expected and pass through this expected position to move from an underestimate to an overestimate of the mismatch. In Fig. 9 we can see one main peak apart from the substrate peak and for cladding layer thicknesses below 0.001 μm, the "sandwiched" layer behaves as a single 0.2-μm single layer. Therefore, the peak separation corresponds to an underestimate of the mismatch (Fig. 10). For increasing cladding layer thicknesses, we can see that the peak separation increases through the value expected when the claddings are $\sim 0.028\,\mu$m thick, until eventually the cladding dominates the profile.

We observe that for cladding thicknesses $> 0.1\,\mu$m the fringe pattern eventually forms a doublet (Fig. 9) whose splitting gradually reduces with increasing cladding layer thickness, until they merge for thicknesses significantly larger than that for the "sandwiched" layer.

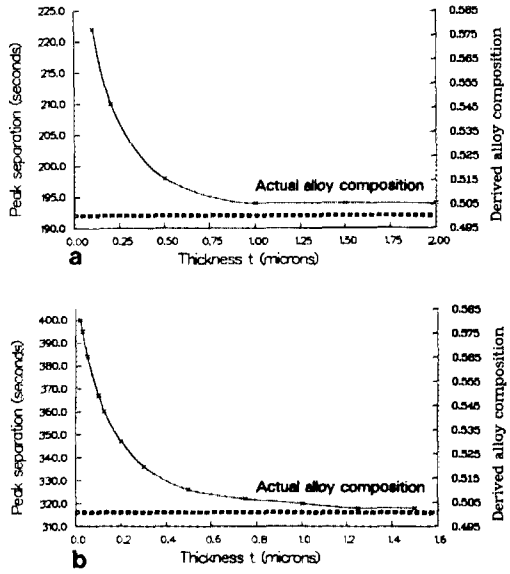

FIG. 7. The variation in peak separation (and its derived alloy composition) for various "sandwiched" $Al_{0.5}Ga_{0.5}As$ layer thicknesses with 0.1-μm $Al_{0.67}Ga_{0.33}As$ cladding layers for the (a) 004 and (b) 224 reflections.

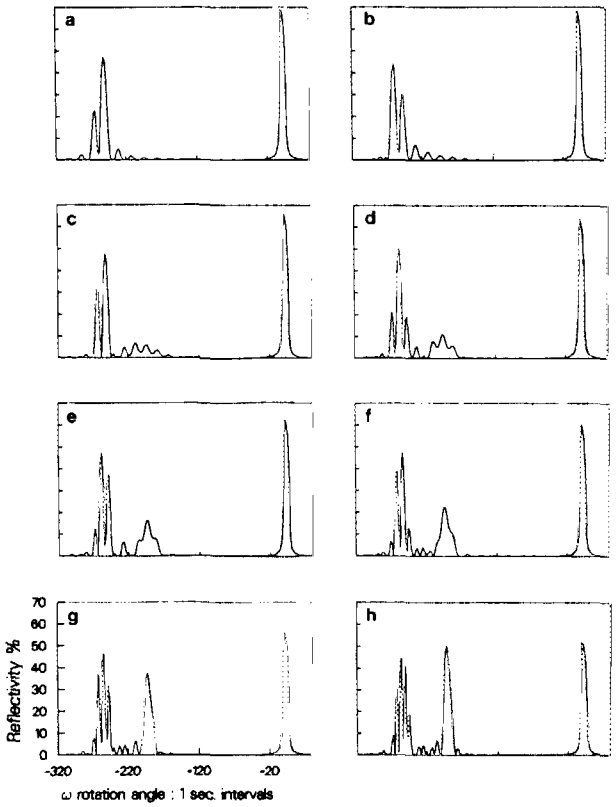

FIG. 8. The change in diffraction profile shape and "sandwiched" $Al_{0.5}Ga_{0.5}As$ layer peak shift with thickness t, for 1-μm $Al_{0.67}Ga_{0.33}As$ cladding layers. (a) $t = 0.1$, (b) 0.2, (c) 0.4, (d) 0.6, (e) 0.8, (f) 1.0, (g) 1.5, and (h) 2.0 μm, for the reflection (Cu$K\alpha$).

Examples of this shifting of layer peaks have been given by Fewster,[3,10] where a good fit to the diffraction profiles was obtained by simulation, and the peak separation method would have given the wrong value of mismatch. To test that this is a real effect and not a peculiarity of the modeling theory, a single $Al_x Ga_{1-x}As$ ($x \sim 0.24$) layer grown by molecular-beam epitaxy on a GaAs substrate was analyzed. The diffraction profile for the 004 reflection and the best-fit simulated profile ($x = 0.235$) are given in Fig. 11(a). The layer was then etched back to 0.22 μm. The layer thickness for a small region close to the diffraction measurement was determined with a surfometer, after etching through to the substrate and detecting the loss of the Al absorption in the photovoltage signal. The diffraction profile was then remeasured. The shift in the layer peak is observed, and for the same composition (mismatch) the simulated profiles agree very closely with the experimental profiles [Fig. 11(b)]. The layer thickness determined by profile fitting was 0.21 μm. The composition derived is 0.235 in x and compares with the photovoltage measurement of 0.245. The small discrepancy in x can be accommodated by choosing a position other than the midpoint of the absorption edge in the photovoltage signal.[11]

An example of peak shifting for an $In_{0.524}Ga_{0.476}As$ layer on an InP substrate is given in Fig. 12, and with this particular example would give rise to a 10% error in the mismatch for a 0.2-μm layer, when derived from the peak separation.

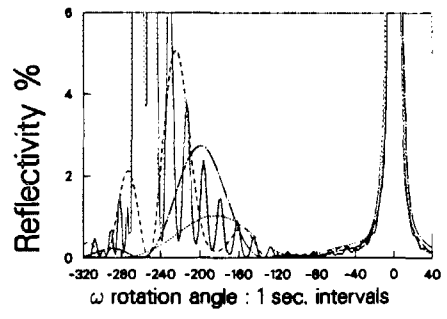

FIG. 9. The change in diffraction peak profile for a 0.2-μm $Al_{0.5}Ga_{0.5}As$ layer cladded by $Al_{0.67}Ga_{0.33}As$ layers of thicknesses 0.001 (dot), 0.05 (dot-dash), 0.1875 (dash), and 1.0 (solid) μm, for the 004 reflection (Cu$K\alpha$).

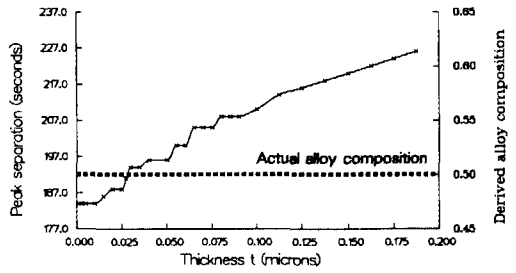

FIG. 10. The change in peak separation as the $Al_{0.67}Ga_{0.33}As$ cladding layers are changed in thickness for a fixed "sandwiched" $Al_{0.5}Ga_{0.5}As$ layer of 0.2 μm for the 004 reflection 004 (Cu$K\alpha$).

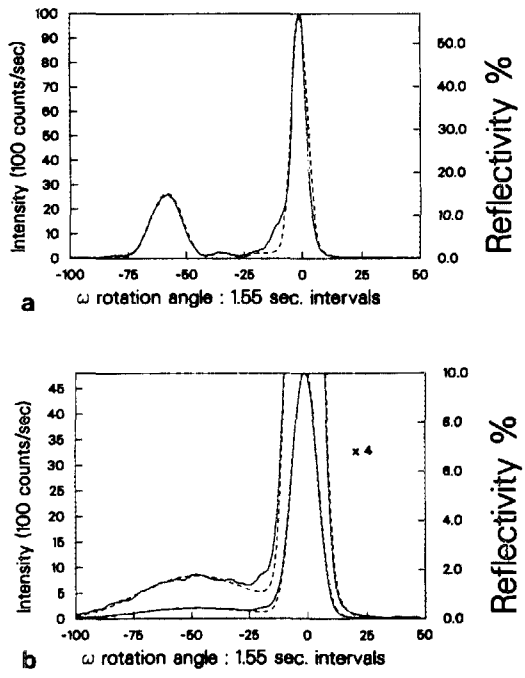

FIG. 11. A comparison between the 004 observed and simulated diffraction profiles for a single $Al_{0.235}Ga_{0.765}As$ layer (a) before etching (0.75 μm) and (b) after etching to 0.21 μm. Both profiles have been convoluted with a rectangular function to account for the sample curvature, which was different before and after etching. The observed data were collected on an APEX goniometer with a four crystal reflection monochromator. The small shoulder on the low angle side of the substrate peak is a feature sometimes observed for this substrate material.

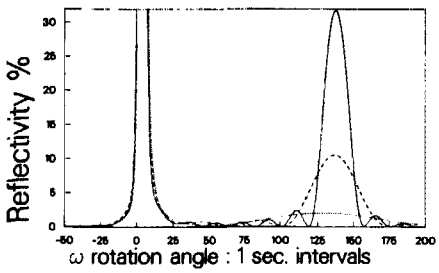

FIG. 12 The 004 (Cu$K\alpha$) simulated diffraction profile from a single $In_{0.524}Ga_{0.476}As$ layer of thickness t on an InP substrate for $t = 1.0$ (solid), 0.5 (dash), and 0.2 (dot) μm showing peak shifting with reduced layer thickness.

IV. CONCLUSIONS

This paper has outlined the problems associated with determining the lattice mismatch from thin epitaxial layers by the peak separation method, despite the fact that their interpretation appears initially to be straightforward. The examples illustrated were given for the AlGaAs system, although we have observed these effects in other systems since it is a diffraction effect and not a consequence of any peculiar material properties. To include the full range of possibilities is unnecessary, but what is important is that the diffraction profiles should be simulated to determine the mismatch for all structures with layer thicknesses below ~ 1–$2\ \mu$m.

It must be remembered that multiple quantum well and superlattice structures will diffract as an average alloy, with additional satellite peaks, therefore it is the total repeat structure thickness that is important, not the individual layer thicknesses for the purpose of determining the mismatch. The profiles illustrated in this paper also give a good indication of the sensitivity of x-ray diffraction methods for the determination of layer thicknesses.

ACKNOWLEDGMENTS

The authors are very grateful to James Bellchambers for etching the layer and carrying out the photovoltage measurements as an independent check of the profile simulation method, and to Tom Foxon for growing the layer.

[1]E. Estop, A. Izrael, and M. Sauvage, Acta Crystallogr. A **32**, 627 (1976).
[2]W. J. Bartels and W. Nijman, J. Cryst. Growth **44**, 518 (1978).
[3]P. F. Fewster, Philips J. Res. **41**, 268 (1986).
[4]B. K. Tanner and M. J. Hill, Adv. X-Ray Anal. **29**, 337 (1986).
[5]S. Takagi, Acta Crystallogr. **15**, 1311 (1962); J. Phys. Soc. Jpn. **26**, 1239 (1969).
[6]D. Taupin, Bull. Soc. Fran. Miner. Cryst. **87**, 469 (1964).
[7]M. Baudet, O. Regreny, G. Dupas, P. Auvray, M. Gauneau, A. Regreny, and G. Talalaeff, Mater. Res. Bull. **18**, 123 (1983).
[8]T. Vreeland and B. M. Paine, J. Vac. Sci. Technol. A **4**, 3153 (1986).
[9]M. A. G. Halliwell, J. Juler, and A. G. Norman, Inst. Phys. Conf. Ser. No. **67**, 365 (1983).
[10]P. F. Fewster, in *NATO Advanced Research Workshop: Thin-Film Growth Techniques for Low Dimensional Structures*, edited by R. Farrow, S. Parkin, P. J. Dobson, J. Neave, and A. Arrott (Plenum, London, 1987).
[11]P. Blood, Semicond. Sci. Technol. **1**, 1 (1986).